RJ 5681 (57180) 6/3/87
Physics

(4)

Research Report

OVERVIEW OF PHOTOTHERMAL SPECTROSCOPY

A. C. Tam
IBM Research
Almaden Research Center
650 Harry Road
San Jose, California 95120-6099

IBM Research Division
Yorktown Heights, New York • San Jose, California • Zurich, Switzerland

SECURITY CLASSIFICATION OF THIS PAGE (When Data Entered)

REPORT DOCUMENTATION PAGE		READ INSTRUCTIONS BEFORE COMPLETING FORM
1. REPORT NUMBER 39	2. GOVT ACCESSION NO.	3. RECIPIENT'S CATALOG NUMBER
4. TITLE (and Subtitle) OVERVIEW OF PHOTOTHERMAL SPECTROSCOPY		5. TYPE OF REPORT & PERIOD COVERED Technical Report 6. PERFORMING ORG. REPORT NUMBER
7. AUTHOR(s) A. C. Tam		8. CONTRACT OR GRANT NUMBER(s) N00014-83-C-0170
9. PERFORMING ORGANIZATION NAME AND ADDRESS International Business Machines, Corp. 650 Harry Road San Jose, CA 95120		10. PROGRAM ELEMENT, PROJECT, TASK AREA & WORK UNIT NUMBERS NR 633-844
11. CONTROLLING OFFICE NAME AND ADDRESS Office of Naval Research 800 N. Quincy Street Arlington, VA 22217		12. REPORT DATE June 1987 13. NUMBER OF PAGES 46
14. MONITORING AGENCY NAME & ADDRESS(if different from Controlling Office)		15. SECURITY CLASS. (of this report) 15a. DECLASSIFICATION/DOWNGRADING SCHEDULE

16. DISTRIBUTION STATEMENT (of this Report)

This document has been approved for public release and sale; its distribution is unlimited

17. DISTRIBUTION STATEMENT (of the abstract entered in Block 20, if different from Report)

"Overview of Photothermal Spectroscopy", Chapter 1, *Photothermal Investigations of Solids and Fluids*, Edited by Jeff A. Sell, Academic Press, NY, (in press, 1988).

18. SUPPLEMENTARY NOTES

19. KEY WORDS (Continue on reverse side if necessary and identify by block number)

Photothermal, spectroscopy, review, overview, probe beam, refraction, refractive index, photoacoustic, nondestructive materials evaluation, flow, velocity, flame diagnostics.

20. ABSTRACT (Continue on reverse side if necessary and identify by block number)

This article provides an overview of photothermal techniques to probe materials with the emphasis on the use of probe-beam refraction techniques to detect photothermal refractive-index gradients. Physical insights into the quantification of the photothermal signal for important cases are provided, significant application areas are reviewed, and recent literature is surveyed.

DD FORM 1 JAN 73 1473 EDITION OF 1 NOV 65 IS OBSOLETE
S/N 0102-LF-014-6601

SECURITY CLASSIFICATION OF THIS PAGE (When Data Entered)

RJ 5681 (57180) 6/3/87
Physics

OVERVIEW OF PHOTOTHERMAL SPECTROSCOPY

A. C. Tam

IBM Research
Almaden Research Center
650 Harry Road
San Jose, California 95120-6099

ABSTRACT: This article provides an overview of photothermal techniques to probe materials with the emphasis on the use of probe-beam refraction techniques to detect photothermal refractive-index gradients. Physical insights into the quantification of the photothermal signal for important cases are provided, significant application areas are reviewed, and recent literature is surveyed.

OVERVIEW OF PHOTOTHERMAL SPECTROSCOPY

A. C. Tam

IBM Almaden Research Center, 650 Harry Road, San Jose, California 95120-6099

I. INTRODUCTION

Photothermal (PT) generation refers to the heating of a sample due to the absorption of electromagnetic radiation. Such radiation exciting the sample can be in the optical range, as well as in other ranges (X-ray, ultraviolet, infrared, microwave and radio frequency). Furthermore, effects similar to PT generation can be produced by other types of excitation beams (electron, proton, ions, *etc.*) instead of an electromagnetic beam. PT generation is an example of energy conversion, and has, in general, three types of applications, namely, (a) PT material probing, (b) PT material processing, and (c) PT material destruction. Thus, type (a) applications cause no sample modification, type (b) applications cause the sample to change to another useful form, and type (c) applications render the sample useless. The temperatures involved also generally increase in this order. This article is only concerned with type (a) applications of PT generation; PT material probing is based on the ideas shown in Fig. 1. Optical excitation of a sample can result in the production of several forms of energy: heat, luminescence, chemical energy or electrical energy. The heat can be produced promptly, or at various time delays due to energy transfer mechanisms. All these resulting energy forms must add up to equal the absorbed optical energy; in other words, the various de-excitation branches shown in Fig. 1 are "complementary."

PT material probing or characterization techniques generally rely on the use of high-sensitivity detection methods to monitor the effects caused by PT heating of a sample. Such possible effects are indicated in Fig. 2. Many of these PT effects occur

simultaneously, *e.g.*, PT heating of a sample in air will produce temperature rise, photoacoustic waves and refractive-index changes in the sample and in the adjacent air, infrared thermal radiation changes, *etc.*, at the same time. Thus, the choice of a suitable PT effect for detection will depend on the nature of the sample and its environment, the light source used, and the purpose of the measurement. This article provides an overview of the experiment arrangements and detection schemes for the various PT effects, and gives a summary of possible applications. Emphasis is given on the use of probe-beam refraction schemes to detect PT refractive-index gradients, and approximate analytical solutions for some typical configurations are provided to show how the observed beam deflection signal depends on various parameters, including delayed heat release due to a long thermal de-excitation time constant. Literature citations are not intended to be exhaustive: rather, only some of the most recent and representative work in this field is provided here. More details and earlier work are found in other chapters in this book, as well as in other reviews (*e.g.*, Tam, 1986; Bialkowski, 1986; Rose *et al.*, 1986).

II. PT DETECTIONS AND APPLICATIONS

Detection methods for various PT effects are summarized in Table I. These detection methods can either be applied to the sample itself, or to the "coupling fluid" adjacent to a condensed sample. (We generally assume that only the sample absorbs the incident light, but not the adjacent coupling fluid, although Low *et al.* (1986) has considered a more complicated case of absorbing coupling gas.) We shall call the former case "direct PT detection," and the latter case "indirect PT detection." All the PT detection schemes require a modulation in the excitation light (or at least a step change). Such a modulation can be in the form of short intense pulses separated by long dark periods (so-called "pulsed PT detection") or continuous train of pulses at nearly 50% duty cycle (so-called continuous-modulated PT detection). The former detection scheme is typically in the "time-domain" where the PT signal magnitude and shape after the pulse excitation is recorded, while the latter detection scheme is typically in the

"frequency-domain" where the PT signal magnitude and phase are phase-sensitive detected with respect to the excitation. Details and examples of the various PT detection are given below.

A. Temperature Rise

The most direct method for measuring PT heating is the monitoring of the rise in temperature; this is sometimes called "optical calorimetry" or "laser calorimetry," since a laser beam is frequently used for excitation. To detect the laser-induced temperature rise, thermocouples or thermisters have been used, as indicated in Fig. 3a (Brilmyer *et al.*, 1977; Bass *et al.*, 1979; Bass and Liou, 1984), and pyroelectric detectors with higher sensitivity have also been exploited, as shown in Fig. 3b (Baumann *et al.*, 1983; Coufal, 1984). Even absorption spectroscopy can be used to detect the rise in temperature if the corresponding Boltzmann molecular population change can be analyzed (Zapka and Tam, 1982a).

There are advantages and disadvantages of using a temperature sensor to detect PT temperature rise directly rather than using other detection methods described later. The main advantage is that absolute calibration is readily available, *i.e.*, the observed temperature rise can be directly measured and related to physical parameters like absorption coefficients. The disadvantages are that response is usually slow, and sensitivity is typically low compared to other methods; furthermore, in what is basically a "dc method," heat leakage from the sample must be minimized by elaborate thermal isolation. However, Coufal (1984) and Coufal and Hefferle (1985) have shown that fast risetime and high sensitivity for a thin-film sample is possible if it is directly coated onto a thin-film pyroelectric detector.

B. Pressure Change

Pressure variations or modulations resulting form the absorption of modulated light by a sample is usually referred to as "photoacoustic" (PA) or "optoacoustic" (OA) generation. PA generation mechanisms include electrostriction, thermoelastic

expansion, volume changes due to photochemistry, gas evolution, boiling or ablation, and dielectric breakdown, with the PA generation efficiency η (*i.e.*, acoustic energy generated/light energy absorbed) generally increases in this order. For electrostriction and for thermal expansion (also called thermoelastic) mechanisms, η is small, often on the order of 10^{-12} to 10^{-8}, while for breakdown mechanisms, η can be as large as 30% (Teslenko, 1977). PT generation *via* thermoelastic expansion, where η is small, is the most common mechanism used in PA spectroscopy. To get a qualitative spectrum of a sample, the wavelength of the excitation beam is scanned, and the corresponding magnitude of the acoustic signal normalized by the excitation pulse energy is measured to provide an "excitation spectrum," called a PA spectrum. To quantify this PA spectrum, the various other "branching ratios" for the de-excitation in the excitation wavelength range (see Fig. 1) must be accounted for.

As discussed for the general case of PT generation, PA generation can be classified as either direct or indirect. In direct PA generation (Fig. 4), the acoustic wave is produced in the sample where the excitation beam is adsorbed. In indirect PA generation (Fig. 5), the acoustic wave is generated in a coupling medium adjacent to the sample, usually due to heat leakage and sometimes also due to acoustic transmission from the sample; here, the coupling medium is typically a gas or a liquid, and the sample is a solid or a liquid.

Extensive reviews of the application of PA detection for spectroscopy and other measurements have been given in the literature, *e.g.*, Rosencwaig (1980), Patel and Tam (1981), and Tam (1986).

C. Refractive Index Gradients

PT heating of a sample can produce Refractive Index Gradient (RIG) in the sample (direct effect) or in an adjacent "coupling fluid" (indirect effect). Also, there are two types of RIG produced by the PT heating of the sample, namely, a "thermal RIG" and an "acoustic RIG." The thermal RIG is produced by the decreased density of the

medium (sample or coupling fluid) caused by the local temperature rise, decays in time following the diffusional decay of the temperature profile, and remains near the initial optically excited region. The acoustic RIG is associated with the density fluctuation of the medium caused by the propagation of the PA wave, decays in propagation distance following the attenuation of the PA wave, and travels at the acoustic velocity away from the initial optically excited region. Thermal RIG and acoustic RIG are related, and can be used to measure similar parameters, like optical absorption coefficient, temperature, or flow velocity of the sample. However, thermal diffusivity can only be measured by the time evolution of the thermal RIG, and acoustic velocity and attenuation can only be measured by the spatial dependence of the acoustic RIG. Also, at distances farther than several thermal diffusion lengths from the excitation region, only acoustic RIG can be detected. In general, thermal RIG provides a larger signal compared to acoustic RIG, which, however, can have narrower temporal profile and be detectable far away from the excitation region.

1. Thermal RIG

The thermal refractive-index gradient generated by the excitation beam affects the propagation of an optical beam in its vicinity, including its own propagation, resulting in the well-known effect of "self-defocusing" or "thermal blooming." Self-defocusing generally occurs instead of self-focusing because the derivative of the refractive index with respect to temperature is usually negative, so that the temperature gradient results in a negative lens. The thermal RIG also affects the propagation of another weak "probe" beam in the vicinity of the excitation beam. Thus, thermal RIG can be monitored either by self-defocusing or by probe-beam refraction (PBR). Leite *et al.* (1964) have first shown that self-defocusing of the excitation beam provides a sensitive spectroscopic tool, and Solimini (1966) later gave a quantitative theory for this application. Swofford *et al.* (1976) have shown that the PBR method with an additional collinear probe beam provides higher sensitivity than the single-beam self-defocusing method; this is called "thermal lensing" spectroscopy using a probe beam. Kliger (1980)

and Bialkowski (1985) have reviewed the spectroscopic applications and analyzed the aberration effects of the thermal lens.

The PBR technique for probing the refractive-index gradient need not employ collinear beams as in the thermal lens experiment. A probe beam that is parallel to, but displaced from, the excitation beam can also be used (see Fig. 6a). Boccara *et al.* (1980) and Jackson *et al.* (1981a) have pointed out that the PBR method, using beams with appropriate displacements, can have higher sensitivity than thermal lens spectroscopy if the probe is positioned at the maximum refractive-index gradient, which is situated at approximately one beam radius from the axis of the excitation beam; their work indicated that an absorption fraction of 1 part in 10^8 can be detected.

In general, the probe beam need not even be parallel to the excitation beam. Although the parallel configuration with a displacement of one beam radius gives the largest probe deflection, this configuration may not always be possible. For example, high spatial resolution measurements necessitate the use of "crossed" beam (Fig. 6b). Also, for opaque samples, orthogonal PBR detection is generally needed since no transmission through the sample is possible (Fig. 6c).

Since the detection of thermal RIG has been extensively used in PT spectroscopy and materials probing, we shall give more detailed description of the theoretical derivations of typical cases of parallel PBR and perpendicular PBR, and their applications. To make the mathematical forms to be simple and analytical so as to provide physical insights, certain conditions on the sample and optical arrangements are imposed. More general cases of PBR for monitoring the thermal RIG can be done by numerical computations (Rose *et al.*, 1986) or by ray-tracing (Sell, 1987). While PBR measurements discussed here are all "linear" with respect to the excitation intensity, nonlinear effects can sometimes be significant (Wetsel and Spicer, 1986; Bialkowski, 1985, Bialkowski and Long, 1987; Long and Bialkowski, 1985).

(a) Parallel PBR

We derived here the theoretical formula for the parallel PBR deflection angle φ (Fig. 6a) for short pulsed excitation and fast thermal de-excitation and a narrow probe beam at a radial distance r from the axis of the excitation beam with a Gaussian profile given by

$$E(r) = \frac{2E_0}{\pi a^2} \exp(-2r^2/a^2), \tag{1}$$

where E_0 is the incident pulse energy of the excitation beam, a is the excitation beam $(1/e^2)$-radius, and E(r) is the energy density at r. The corresponding temperature gradient at r immediately after the short pulsed excitation is

$$\frac{dT}{dr} = \frac{-8E_0\alpha}{\rho C_p \pi a^2} \frac{r \exp(-2r^2/a^2)}{a^2}, \tag{2}$$

where ρ = density, C_p = specific heat, and α = absorption coefficient (assumed small). For small probe deflection φ, geometrical optics gives

$$\frac{\varphi n_0}{l} = \frac{dn}{dr} = \frac{dn}{dT} \frac{dT}{dr}, \tag{3}$$

where l is the optical path length, and n is the sample refractive index of ambient value n_0. Combining Eqs. (2) and (3), we have

$$\varphi(r) = \frac{l}{n_0} \frac{dn}{dT} \frac{(-8E_0\alpha)}{\rho C_p \pi a^2} \frac{r \exp(-2r^2/a^2)}{a^2}. \tag{4}$$

Equation (4) is basically the same as given by Boccara *et al.* (1980) or by Rose *et al.* (1986). We see from Eq. (4) that the probe-beam deflection $\varphi(r)$ depends linearly on the temperature derivative of the refractive index, and linearly on α (for weak absorption), and is maximum at $r = a/2$.

Note that the parallel PBR angle $\varphi(r)$ given in Eq. (4) for the probe located at displacement r form the pump beam axis is valid only if the following conditions are satisfied: (a) weak absorption, (b) short excitation duration, (c) narrow probe beam, (d) sample thermal de-excitation time τ is small, (e) no thermal diffusion (*i.e.*, observation shortly after excitation), and (f) no flow of the sample. In case where condition (e) is not satisfied, *i.e.*, observation is made at time t after the short excitation pulse, Eq. (4) is still valid if the following substitution for the excitation radius a is made:

$$a^2 \longrightarrow (a^2 + 8Dt) \tag{5}$$

where D is the thermal diffusivity. Furthermore, if a flow velocity V_z exists, where z is the direction from the pump beam to the probe beam, Eq. (4) is still valid with the following substitution for the beam-separation parameter r:

$$r \longrightarrow (z - v_z t)\,. \tag{6}$$

Thus. in the more general case of parallel PBR observed at a delay time t in presence of a flow v_z, the deflection angle $\varphi(z,t)$ is given by

$$\varphi(z,t) = \frac{l}{n_0}\,\frac{dn}{dT}\,\frac{(-8E_0\alpha)(z - v_z t)\exp[-2(z - v_z t)^2/(a^2 + 8Dt)]}{\rho C_p \pi (a^2 + 8Dt)^2} \tag{7}$$

which agrees essentially with the "traveling thermal lens" deflection angle derived by Sontag and Tam (1956b), in which a factor of 2 was inadvertently missed. Note that Eq. (7) still requires that conditions (a) and (d) stated after Eq. (4) are satisfied.

(b) Perpendicular PBR

Consider the geometry of Fig. 6b where the pump beam goes at direction y, probe beam goes at direction x, and the probe axis and pump axis are separated by a distance z. We again assume that conditions (a) to (c) listed after Eq. (4) are valid. However, we generalize here to examine the effects of finite thermal de-excitation time τ and finite observation time t after the short-duration excitation. The flow velocity is assumed to

be zero; however, any flow v_z in the z-direction can again be accounted for by the following substitution

$$z \longrightarrow (z - v_z t) \tag{8}$$

For cylindrical symmetry, the temperature rise T(r,t) will obey the following differential equation

$$\frac{\partial^2 T}{\partial r^2} + \frac{1}{r}\frac{\partial T}{\partial r} - \frac{1}{D}\frac{\partial T}{\partial t} = -\frac{N(r', t')h\nu}{D\rho C_p \tau}\exp(-t'/\tau), \tag{9}$$

where r is the radial coordinate, D is the thermal diffusivity, N(r't') is the concentration of excited molecules, hν is the photon energy, ρ is the density, C_p is the specific heat, and τ is the thermal relaxation time. We have assumed that the heat generation process is characterized by the single time constant τ. The density of excited state molecules after excitation by a short-duration Gaussian shaped pump beam with beam parameter a is given by

$$N(r,t) = \frac{2\alpha E_0}{\pi h\nu(a^2 + 8D_m t)}\exp\frac{-2r^2}{a^2 + 8D_m t} \tag{10}$$

where α is the absorption coefficient, E_0 is the pump pulse energy, hν is the photon energy and D_m is the molecular diffusivity. Here, we include the consideration of the diffusion of excited molecules out of the production zone; this may be important, as molecular and heat transport in gases are of comparable magnitude. In Eq. (9), the heat source term Q(r', t') has been expressed as

$$Q(r', t') = \frac{N(r', t')h\nu\exp(-t'/\tau)}{\tau} \tag{11}$$

For cylindrical symmetry, the temperature rise T caused by the pulsed linear heat source Q(r', t') has been calculated by Carslaw and Jaeger (1959) as

$$T(r,t) = \int_0^t dt' \int_0^\infty 2\pi r' dr' Q(r', t') G(r', r, t - t') \tag{12}$$

where the Green's function $G(r', r, t - t')$ for a cylindrical shell of radius r' is given by

$$G(r', r, t - t') = \frac{1}{4\pi K(t - t')} I_0\left(\frac{rr'}{2D(t - t')}\right) \exp\left(-\frac{r^2 + r'^2}{4D(t - t')}\right) \tag{13}$$

K is the thermal conductivity, D is the thermal diffusivity of the medium, and I_0 is a modified Bessel function. By using Eqs. (10), (11), and (13), the integral in Eq. (12) can be evaluated to obtain the time dependent temperature distribution T as

$$T(r,t) = \frac{2\alpha E_0}{\pi C_p \rho \tau} \int_0^t dt' \exp\frac{(-t'/\tau)}{A(t, t')} \exp\left(\frac{2r^2}{A(t, t')}\right) \tag{14}$$

where $A(t, t')$ is given by

$$A(t, t') = a^2 + 8D_m t' + 8D(t - t'). \tag{15}$$

From Eqs. (14) and (15), it is clear that for fast thermal relaxation so that $\tau << a^2/8D_m$ and $\tau << a^2/8D$, the effect of molecular diffusion becomes negligible; in this case, we can put $D_m \approx 0$ and take the slower time-varying terms outside the integral in Eq. (14) to obtain the simple solution for the temperature distribution

$$T(r, \tau) = \frac{2\alpha E_0}{\pi \rho C_p} \frac{[1 - \exp(-t/\tau)]}{(a^2 + 8Dt)} \exp[-2r^2/(a^2 + 8Dt)]. \quad \text{(short } \tau\text{)} \tag{16}$$

The perpendicular PBR angle $\psi(z,t)$ for the geometry of Fig. 6b is given by

$$\psi(z,t) = \frac{1}{n_0} \frac{\partial n}{\partial T} \int_{-\infty}^{\infty} \frac{\partial T}{\partial z} dx. \tag{17}$$

Substituting Eq. (14) into Eq. (17), we obtain the time-dependent perpendicular PBR angle

$$\psi(z,t) = \frac{1}{n_0}\,\frac{\partial n}{\partial T}\,\frac{(-8\alpha E_0 z)}{\sqrt{2\pi}\,\tau\rho C_p}\int_0^t dt'\,\frac{\exp(t'/\tau)\exp[-2z^2/A(t,t')]}{A(t,t')^{3/2}}\,. \qquad (18)$$

Again, for $\tau << a^2/8D_m$ and $\tau << a^2/8D$, this simplifies as for the case of T(r,t) given by Eq. (16) to be:

$$\psi(z,t) = \frac{1}{n_0}\,\frac{\partial n}{\partial T}\,\frac{(-8\alpha E_0 z)}{\sqrt{2\pi}\,\rho C_p}\,\frac{(1-e^{-t/\tau})}{(a^2+8Dt)^{3/2}}\exp\left(-\frac{2z^2}{a^2+8Dt}\right). \quad \text{(short } \tau\text{)} \quad (19)$$

The calculated deflection signals, ψ for a few pump probe separations z for fast thermal relaxation (*i.e.*, $\tau \longrightarrow 0$), are shown in Fig. 7a. The signal shape expected for a "slow" component (*i.e.*, finite τ) is shown in Fig. 7b, which is taken from the work of Sontag *et al.* (1987).

As noted earlier, Eqs. (18) and (19) can be applied to a flowing fluid sample in the z-direction (*i.e.*, perpendicular "traveling thermal lens" case) by the substitution of Eq. (8) in Eqs. (18) or (19).

In general, the pulsed pump beam may not be cylindrically symmetric with a Gaussian beam shape. We can estimate the importance of this effect by examining the case where the pump beam has a Gaussian intensity distribution with beam parameter a in the z-direction, but possesses a rectangular intensity distribution of width a_1 in the x-direction (see coordinate system in Fig. 6b. In addition, we assume that $a_1 >> a$, such that heat flow in the x-direction can be neglected. In this limit, we can treat the heat flow in one dimension only. We will show that for this case, the same probe deflection as for cylindrical symmetry case is obtained, indicating that the intensity distribution of the pump beam in the x-direction is unimportant for PBR.

Using the result for a plane source, we can set up the general solution as

$$T(z,t) = \int_0^t dt' \int_{-\infty}^{\infty} dz' G(z', z, t - t') Q(z', t') \tag{20}$$

where

$$G(z', z, t - t') = \frac{1}{2\sqrt{\pi D(t - t')}} \tag{21}$$

and

$$Q(z', t') = \frac{\sqrt{2}\,\alpha E_0 \exp[-2z'^2/(a^2 + 8D_m t')]}{\rho C_p \sqrt{\pi}\,\tau a_1 \sqrt{a^2 + 8D_m t'}} \exp\left(-\frac{t'}{\tau}\right). \tag{22}$$

Equations (20)-(22) can be integrated to yield

$$T(z,t) = \int_0^t dt' \frac{\sqrt{2}\,\alpha E_0}{\sqrt{\pi}\,\tau a_1 \rho C_p} \exp\frac{(-t'/\tau)}{\sqrt{A(t, t')}} \exp\left(-\frac{2z^2}{A(t, t')}\right). \tag{23}$$

The perpendicular PBR angle ψ is again derived by inserting Eq. (23) into Eq. (17), from which the same result as in Eq. (18) is obtained. This can intuitively be understandable, since in the present perpendicular beams arrangement, the interaction length of the probe beam with the thermal lens increases with a larger excitation beam waist in the x-direction, and this effect counteracts the smaller RIG. We, therefore, conclude that the intensity distribution of the pump beam in the probe direction is of minor importance in perpendicular PBR experiments if the intensity distribution of the pump beam is Gaussian along the z-direction; Eq. (18) or (19) should adequately describe the perpendicular PBR angle ψ.

(c) Application of PBR Due to Thermal RIG

Numerous applications of PBR detection of thermal RIG have been recently reported in the literature; such applications include spectroscopy, analytical application and trace detection, imaging and defect detection, and flow or combustion diagnostics. This great current interest arises because of the high sensitivity and spatial and temporal resolution achievable with this technique together with the desirable noncontact nature of the detection method. More detailed considerations have been given by Rose *et al.* (1986), Murphy and Wetsel (1986), Bialkowski (1986), and Morris and Peck (1986).

Spectroscopy. Murphy and Aamodt (1980) and Jackson *et al.* (1981a) have calculated the probe-beam deflection for cases of cw or pulsed excitation with either perpendicular or parallel probe. Jackson *et al.* (1981a) have experimentally verified some of the predictions of their theory. For example, they have used PBR spectroscopy to measure the optical absorption of benzene at 607 nm due to the sixth harmonic of the C − H stretch. From their experimental results for a 0.1% solution of benzene in CCl_4, they concluded that the PBR method can detect an absorption coefficient of 2×10^{-7} cm^{-1} for a 1-mJ pulsed-excitation laser with the detection limit being mainly due to the pointing instability of the HeNe probe laser. Jackson *et al.* (1981b) have also reported the measurement of absorption spectra of crystalline and amorphous Si by photothermal PBR spectroscopy. Orthogonal PT PBR (or "mirage" probing) has been used for novel spectroscopic applictions by Fournier *et al.* (1981), Murphy and Aamodt (1981), and Low *et al.* (1982). In addition, orthogonal PBR (with the probe intersecting the pump beam inside the sample) has been used by Dovichi *et al.* (1984) for PT microscopy applications. Nickolaisen and Bialkowski (1985) have used a pulsed infrared laser for thermal lens spectroscopy of a flowing gas sample. There are more recent reports on spectroscopic measurements on thin films (Dadarlat *et al.*, 1986; Hata *et al.*, 1986) and on adsorbed species (Morterra *et al.*, 1985). The use of "hexane soot" as the reference absorber for PT spectroscopy has been investigated (Low, 1985).

Fourier transform (FT) techniques have been extensively applied to PBR spectroscopy for efficient spectroscopic measurements and signal-to-noise improvement. Earlier work was reported by Fournier *et al.* (1981) who showed PBR FT spectroscopy for absorption and dichroism measurements and obtained three orders of magnitude improvement in sensitivity over conventional PA spectroscopy. Low *et al.* (1984) have combined the infrared Fourier-multiplexed excitation technique with photothermal PBR detection for spectroscopy of "difficult" samples like polymers, fabrics, paper, and bones. Other PBR FT spectroscopy applications include studies of thin films (Roger *et al.*, 1985), electrodes (Crumbliss *et al.*, 1985), solid/liquid interface (Varlashkin and Low, 1986a,b), and infrared spectral depth profiling (Varlashkim and Low, 1986c). Much consideration on instrumentation is given by Mandelis and co-workers (Mandelis, 1986; Mandelis *et al.*, 1986a,b). Besides FT, other multiplexed techniques like Hadamard transform have been reported (Fotiou and Morris, 1987).

Analytical Applications. This is a particular case of spectroscopic measurement to determine compositions (perhaps in small amounts). Numerous reports have been published recently. Long and Bialkowski (1985) have shown the use of PBR PT spectroscopy for trace gas detection at the sub-part-per-billion level, and Fung and Lin (1986) and Tran (1986) have done trace gas analysis *via* intracavity PBR spectroscopy. Analytical applications for solutions (Uejima *et al.*, 1985), powder layer (Tamor and Hetrick, 1985), surfaces (Field *et al.*, 1985), and black inks on paper (Varlashkin and Low, 1986a) have also been reported. Comparisons of detection limits by PT spectroscopy with other types of analytical techniques have also been given by Winefordner and Rutledge (1985).

Imaging. Murphy and Aamodt (1980,1981) have demonstrated PT imaging using perpendicular PBR (called the "mirage effect"). Kasai *et al.* (1986) have used PBR for nondestructive materials evaluation, Mundy *et al.* (1985) and Abate *et al.* (1985) have used PBR for coating evaluation, and Baumann and Tilgner (1985) have discussed the theory for the measurement of the thickness of a buried layer. McDonald *et al.* (1986)

have used PBR for imaging "vertical interfaces" in solid and Rajakarunanayake and Wickramasinghe (1986) have demonstrated novel nonlinear PT imaging.

Flow diagnostics. Sontag and Tam (1985b,1986a), Sell (1985), and Weimer and Dovich (1985) have demonstrated "traveling thermal lens" spectroscopy for monitoring flow velocity, temperature, and composition in a flowing fluid. Rose *et al.* (1986) have made a very detailed analysis of the PBR signal shape in a flowing fluid system for applications in combustion diagnostics. Sell and Cattolica (1986) have shown velocity imaging in a flowing gas. Optimization of velocity measurements by such techniques are given by Dasch and Sell (1986) and by Weimer and Dovichi (1985a,b). To show the feasibility of single-pulse measurement of local thermal diffusivity or temperature in a combustion system, Loulergue and Tam (1985) have used a pulsed-excitation CO_2 laser beam and a continuous HeNe probe beam that is parallel to but displaced from the excitation beam for thermal diffusivity measurements in an unconfined hot gas.

Other applications. The use of time-resolved photothermal PBR techniques to detect delayed heat release, for example, due to energy transfers or photochemical reactions is also possible. This has been demonstrated by Tam *et al.* (1985) for the case of photochemical particulate production in a CS_2 vapor induced by a pulsed N_2 laser, where the delayed heat release is attributed to the nucleation and growth of particulates. A delayed peak can be observed in the probe-beam deflection signal when delayed heat release occurs, as shown in Fig. 8; more details on this use of time-resolved PBR for thermal relaxation measurements in chemically active systems are reported by Sontag *et al.* (1987). We also note that PBR can also be used to detect thermal release due to radio-frequency or microwave-frequency excitation, *e.g.*, in ferromagnetic resonance (Netzelmann *et al.*, 1986).

2. *Acoustic RIG*

Similar to the optical probing of the thermal RIG, we can also detect the RIG associated with the PA pulse. The detection of refractive-index variation caused by

acoustic waves is not new; for example, this has been reported by Lucas and Biquard (1932) and Davidson and Emmony (1980). The present discussion is focused on its use for PA detection, which is similar to the above PT detection scheme. This method can be called optical probing of the acoustic refractive-index gradient (OPARIG); it is applicable for "direct detection" inside a material transparent to the probe beam, or to "indirect detection" in a transparent coupling medium adjacent to an opaque sample. Here, the transient deflection of the probe due to the traversal of the PA pulse is detected. By using two or more probe beams at different displacements at different times, acoustic velocity and attenuation of the sample or of the coupling medium can be detected. Quantification of the OPARIG signal S(t) has been given by Sullivan and Tam (1984), using a photodiode with a small active area as a fast deflection sensor (see Fig. 9). When the PA pulse produced by the excitation beam crosses the probe beam, a transient angular deflection (Klein, 1970) φ of the probe is produced,

$$\varphi(r,t) \approx \frac{l}{n_0} \frac{\partial n(r,t)}{\partial r} \propto \frac{\partial P(r,t)}{\partial t} , \tag{24}$$

where n(r,t) is the refractive index of normal value n_0, P(r,t) is the PA pressure, and l is the interaction length of the PA pulse with the probe laser. The small transient probe deflection φ causes the probe beam to move across the detection photodiode. The observed probe-beam deflection signal S(t) from the photodiode is given by

$$S(t) = GI_p'(r_d)L\varphi , \tag{25}$$

where G is a constant depending on the photodiode sensitivity and electronic gain of the detection system, $I_p'(r_d)$ is the lateral spatial derivative of the probe-beam intensity distribution at the photodiode position r_d (with the active area of the photodiode being sufficiently small), and L is the "lever arm" of the probe beam (*i.e.*, distance from the interaction region in the cell to the photodiode). Combining Eqs. (24) and (25), we have

$$S(t) \propto \frac{\partial P(r,t)}{\partial t} , \tag{26}$$

which means that our experimental probe-beam deflection signal is a measure of the *time derivative* of the PA pulse at the probe-beam position. This present discussion assumes that the detection is made sufficiently far away from the excitation region region so that thermal RIG effects are negligible. Sullivan and Tam (1984) have used OPARIG for a reliable determination of PA pulse profiles generated by laser beams of durations in the μsec or nsec regimes to verify the theoretical PA pulse profiles calculated by Lai and Young (1982) and by Heritier (1983).

A novel application of OPARIG for acoustic absorption spectroscopy in gases, to be called "PA spectroscopy of the second kind" (to distinguish it from the well-known first kind concerned with optical absorption spectroscopy) has been reported by Tam and Leung (1984). Here, the acoustic absorption spectrum of a gas sample is obtained by measuring the Fourier spectrum of S(t) at different distance from the PA source; the decay of the Fourier spectrum with propagation distance gives the acoustic absorption spectrum of the gas. Thus, optical monitoring of PA pulse profiles should open up new noncontact ultrasonic velocity, relaxation, and dispersion measurements. For example, chemical reactions, nucleations, precipitations, *etc.*, in a system frequently cause changes in the ultrasonic absorption or dispersion spectra, detectable by monitoring the profiles of the probe-beam deflection signals at several propagation distances.

Zapka and Tam (1982b,1982c) have demonstrated a new application of the laser-induced acoustic source for measurements in a flowing fluid. They show that the flow velocity of a pure particle-free gas (as well as of a liquid) can be measured to an accuracy of 5 cm/sec, and simultaneously the fluid temperature can be obtained to an accuracy of 0.1°C. Such noncontact measurements were not possible previously by other known laser scattering methods (like laser Doppler velocimetry, coherent anti-Stokes Raman scattering, or stimulated Raman-gain spectroscopy). In their experimental arrangement, an acoustic pulse in a flowing air stream is produced at position 0 by a pulsed-excitation laser (Nd:YAG laser, ~10 mJ energy and 10-nsec duration). Three probe HeNe laser beams, 1, 2, and 3, at distances l_1, l_2, and l_3 from 0,

are used to monitor the acoustic pulse arrival times t_1, t_2, and t_3, respectively. The acoustic pulse arrival at each beam is indicated by the transient deflections of the beam and can be detected by using a knife edge and a photodiode of suitable risetime. Zapka and Tam (1982c) have shown that the deflection signals provide enough data to give both the flow velocity and the fluid temperature simultaneously, and at the same time minimizing possible errors due to a blast wave or a shock wave produced at the origin 0.

Note that both the acoustic RIG detection and the thermal RIG detection can be used for noncontact flow, temperature, and composition measurements in fluids. In fact, both the PA and PT deflection (*i.e.*, refraction) can be generally observed with the same experimental setup, with the PA deflection occurring earlier for displaced excitation and probe beams. For flow diagnostics, PT deflection is more suitable for slow flow velocities, and PA deflection is more suitable for fast flows.

3. Other Detection Schemes of RIG produced by PT Generation

We have described only PBR techniques for detecting PT generated refractive-index variations (thermal or acoustic); however, such variations can also be probed by other optical techniques, notably the phase-fluctuation heterodyne interferometry technique (Davis, 1980) and the Moire deflectometry technique (Glatt *et al.*, 1984). Nelson and Fayer (1980) have used two intersecting coherent pump beam for PT generation of a thermal refractive-index grating in a sample, and use a probe beam diffraction scheme to measure the decay of this grating. Also, Williams (1984) has used a high frequency (~ 1 GHz) train of short laser pulses to irradiate an opaque sample adjacent to a gas (Fig. 10), and observed Bragg scattering of a probe beam due to the modulated refractive index in the gas; this method has the interesting application of measuring ultrahigh frequency sound propagation in gases or liquids.

D. Surface Deformation

As for the case of RIG, the deformation of a sample surface due to PT excitation can be of two kinds, thermal deformation and acoustic deformations. While these two deformations are related, the thermal one decays in time as for thermal diffusion, while the acoustic one propagates into the sample bulk and also along the sample surface as bulk and surface acoustic waves, respectively.

1. Thermal Surface Deformation

The PT heating of a surface causes distortions due to thermal expansion. The distortions can be very small, *e.g.*, 10^{-3}Å. However, Amer and co-workers (Amer, 1983; Olmstead *et al.*, 1983, Olmstead and Amer, 1984) have observed that even such small surface deformations can be detected, providing new sensitive spectroscopic applications. This has been called PT displacement spectroscopy.

The technique of photothermal displacement spectroscopy can be understood from Fig. 11. Figure 11a indicates the case when a laser beam of power P and area A chopped at a frequency f is incident on a solid. Let us assume the simple case of weak absorption by a thin coating (of thickness l and absorption coefficient α) on a transparent substrate. The modulated heating is "spread" through a thermal diffusion length μ given by

$$\mu = \left[\frac{D}{\pi f} \right]^{1/2}, \tag{27}$$

where D is the thermal diffusivity of the solid. The average temperature rise ΔT in this thermal diffusion volume can be estimated as

$$\Delta T = \frac{\alpha l P}{2 f \rho C \mu A}, \tag{28}$$

where P/2f is approximately the incident energy in one cycle, αl is the fraction of light absorbed, ρ is the density, and C is the specific heat of the solid. The magnitude of the maximum surface displacement h_0 is estimated as

$$h_0 = \beta\mu\Delta T = \frac{\beta\alpha I P}{2f\rho CA} , \tag{29}$$

where β is the linear thermal expansion coefficient of the solid. We see that the surface displacement is proportional to the coating absorption coefficient α, and hence absorption spectroscopy of the coating can be performed by monitoring the distortion as a function of the excitation laser wavelength. Equation (29) is derived semiquantitatively and shows the correct dependence of h_0 on various parameters: β, P, f, ρ, C, and A for thermally thick samples; detailed analysis are given by Miranda (1983).

Amer and co-workers show that the surface displacement can be conveniently monitored by a probe-beam deflection method indicated in Fig. 11b. The continuous probe is deflected by the deformation, and the displacement S at a detector plane (perpendicular to the probe beam) is given by [see Fig. 11b]

$$S = 2h_x \cos\theta + 2g_x L . \tag{30}$$

Here, the subscript x indicates the location where the probe beam meets the solid surface, h_x is the height of the distortion at x , g_x is the local gradient due to the distortion at x, L is the distance from x to the detector, and θ is the grazing angle of the probe beam. Both h_x and g_x are proportional to h_0 given by Eq. (29) for small distortion. The gradient deflection term ($2g_x L$) can be made much larger than the height deflection term ($2h_x \cos\theta$) by making the optical level arm L sufficiently long.

The advantages of PT displacement spectroscopy for absorption measurements are that it is noncontact and compatible with a vacuum environment. The disadvantages are that it is applicable only to reflective and smooth surfaces, and careful alignment of the probe beam is required. Olmstead and Amer (1984) have used photothermal displacement spectroscopy for measuring absorption at silicon surfaces and have

achieved a new understanding of the surface atomic structure. Karner *et al.* (1985) have used pulsed laser PT displacement spectroscopy for surface analysis.

It is not always possible to totally separate surface deformation effects form the refractive-index gradient effects described in Sec. C. For example, Rosencwaig *et al.* (1983) and Opsal *et al.* (1983) have examined the case of a coated sample (SiO_2 on Si) in which the probe beam can be significantly affected by several PT effects, including deformations of the SiO_2 and of the Si surfaces, refractive-index gradients in the gas and in the SiO_2, optical interference effects in the SiO_2 film, and PT-induced reflectivity variations.

2. Acoustic Surface Deformation

Noncontact optical probing of surface movements due to acoustic waves has been studied by numerous workers because of its important materials testing applications. Earlier reviews were given by Whitman and Korpel (1969) and Stegeman (1976), and a general summary of noncontact ultrasonic transducers for nondestructive testing has been given by Hutchins (1983). The optical detections of PA surface deformation are similar to these earlier work on optical probing of surface acoustic wave; the more commonly used methods are probe-beam deflection, interferometry, and Doppler velocimetry measurements. Review of the optical detection of PA surface wave or deformations are given by Monchalin (1986) and by Sontag and Tam (1986b).

The probe beam deflection measurement of surface acoustic deformation is similar to the method of optical detection of PT surface distortion developed by Amer (1983) described above. It is based on the deflection of a probe beam reflected from the surface. The distinctions between PT distortion and PA distortion may be described as follows: PT distortion is due to the thermal expansion associated with the local temperature rise, follows the temperature decay *via* diffusion, and remains close to the excitation region: PA distortion, on the other hand, propagates at a sound speed away from the excitation region. Only PA monitoring can provide values of sound speed and attenuation. At

distances more than several thermal diffusion lengths away from the excitation regime, only PA distortion can be detected. Sontag and Tam (1985a) have extended the probe-beam deflection technique of Amer (1983) for detecting multiply reflecting PA pulses in a silicon wafer excited by a pulsed N_2 laser. Such noncontact techniques (extending the usefulness of contact PA testing in Tam (1984) and Tam and Ayers (1986)) are useful for fast ultrasonic testing and imaging and for remote sensing of samples that are "inaccessible" (*e.g.*, in a vacuum chamber, in hostile environments, or whenever contamination must be minimized).

Another method of optical sensing of PA surface distortion relies on interferometry. In this case, a probe beam is split into two parts, one being reflected from the sample surface and another from a reference surface. The reflected beams are recombined, and the resultant intensity is monitored. Kino and his associates (Jungerman *et al.*, 1982,1983; Bowers, (1982) have developed a coherent fiber-optic interferometry technique for measuring acoustic waves on a polished or even on a rough surface. Also, Cielo (1981) has described an optical detection method of acoustic waves for the characterization of samples with unpolished surfaces. Palmer *et al.* (1977) have analyzed a Michelson interferometry system for measuring displacement amplitudes in acoustic emission; their analysis was subsequently criticized by Kim and Park (1984). Bondarenko *et al.* (1976), Calder and Wilcox (1980), and Hutchins and Nadeau (1983) have used Michelson interferometry for detecting the PA pulse shape excited by a powerful pulsed laser (*e.g.*, ruby, Nd:glass, or Nd:YAG laser) in metal plates, while Suemune *et al.* (1985) have extended this work to detect photoacoustic vibration in a GaAs plate produced by a focused diode laser beam modulated at ~100 Hz.

Other novel methods for optical sensing of PA surface deformation have been reported, notably the technique of "piezo-reflection" measurement of Eesley *et al.* (1987); they showed that ultrashort PA pulses of picoseconds duration produce observable surface reflectivity changes, thus opening up the possibility of optical ultrasonic measurements in the picosecond domain.

E. Photothermal Radiometry

Photothermal radiometry (PTR) relies on the detection of variations in the infrared thermal radiation emitted from a sample that is excited by an electromagnetic "pump" beam (typically from a laser or from an arc lamp) of varying intensity or wavelength. A simple theory of PTR is given by Nordal and Kanstad (1979). The total radiant energy W emitted from a grey body of emissivity ε and absolute temperature T is given by the Stefan-Boltzmann law

$$W = \varepsilon\sigma T^4 , \tag{31}$$

where σ is the Stefan-Boltzmann constant. Suppose the body is irradiated by an optical pulse of energy E at wavelength λ that is absorbed by the body with an absorption coefficient $\alpha(\lambda)$, resulting in a small temperature rise $\delta T(E, \alpha)$. By Eq. (31), the total radiant energy is increased by

$$\delta W(E, \alpha) = 4\varepsilon\sigma T^3 \delta T(E, \alpha) . \tag{32}$$

If $\delta T(E, \alpha)$ varies linearly with αE, spectroscopic measurement is possible by defining the "normalized" PTR signal S as

$$S(\alpha) = \delta W(E, \alpha)/E . \tag{33}$$

An excitation spectrum called a PTR spectrum can be obtained by monitoring S for various excitation wavelengths λ.

In a typical PTR measurement, the excitation beam (of photons, or more generally, of some form of energy) is either continuously modulated, with about 50% duty cycle, or pulse modulated, with low duty cycle and high peak power. The observation spot can, in principle, be anywhere on the sample; however, the IR emission is usually detected at the excitation spot in a backward direction (called "backscattering PTR"), or from a spot that is "end-on" through the sample thickness from the excitation spot (called "transmission PTR"). Thus, there are four common variations of PTR in

the literature, as classified according to the excitation mode (continuously modulated or pulsed) and to the detection mode (transmission or backscattered). These are summarized in Fig. 12, and some applications published in the literature are reviewed by Tam (1985) and Kanstad and Nordal (1986).

As is a common problem with all other PT monitoring techniques, the PTR signal magnitude normalized to the energy of the excitation pulse is not necessarily proportional to the absorption coefficient of the sample at the excitation wavelength. In other words, the excitation spectrum obtained by measuring the normalized PTR signal as a function of excitation wavelength may not be proportional to the true absorption spectrum. For a semi-infinite sample, this proportionality is true if the sample absorption coefficients at the detected infrared wavelengths are very large compared to those at the excitation wavelengths (see Tam, 1985).

Applications

Early work of PTR was done by Deem and Wood (1963) who used pulsed ruby laser for excitation and transmission radiometric monitoring to perform noncontact thermal diffusivity measurements of nuclear fuel material. Nordal and Kanstad (1978,1981) and Kanstad and Nordal (1986) have extensively investigated the many applications of PTR, causing its modern popularity; they have demonstrated very sensitive spectroscopic absorption measurements, *e.g.*, due to less than a monolayer of molecules on a surface. Moreover, such spectroscopic measurements can be performed on "difficult" samples like powders or materials at high temperature. Using continuously modulated transmission PTR, Busse (1980), Busse and Eyerer (1983), and Busse and Renk (1983) have detected voids inside opaque solids.

Using pulsed transmission PTR, Deem and Wood (1962) have measured thermal diffusivity of "dangerous" materials like nuclear fuels. With pulsed backscattering PTR, Tam and Sullivan (1983) and Leung and Tam (1984a,1984b) have demonstrated several remote-sensing applications, including the measurement of absolute absorption

coefficients, monitoring of layered structure and film thickness, and detection of the degree of aggregation in powdered materials. Using intense pulsed lasers for excitation and single-ended monitoring, such measurements should be possible for samples that are ~1 km away.

There are rapidly expanding interest in PTR mainly because of its remote sensing nature, depth-profiling capability, absolute spectroscopic measurement possibility, and adaptability to measure the spectra of aerosols, powders, and films. Examples of such work include the quantitative measurement of opaque layered structures (Tam and Sontag, 1986; Cielo *et al.*, 1986; Egee *et al.*, 1986; Beaudoin *et al.*, 1986), aerosol and flow measurements (Lin and Campillo, 1985; Sontag and Tam, 1986a), semiconductor defects detection and imaging (Nakamura *et al.*, 1985) and small absorption measurement (Lopatkin *et al.*, 1985).

F. Other PT Changes

Besides the more common PT effects described above that have been extensively used for PT spectroscopy and material testing applications, many other PT effects are possible, especially for special circumstances. For example, large "bimorph" type of mechanical vibrations can be produced for a suitably supported thin plate that is PT excited at one side only (Rousset *et al.*, 1983), and these vibrations, especially large at mechanical resonances, can be detected by probe beam deflection, interferometry, or Doppler velocity methods. Also, modulated PT heating of many types of metal or semiconductor surfaces causes modulated reflectivity changes (Rosencwaig *et al.*, 1985) or transmission and scattering changes (Rosencwaig *et al.*, 1986) which can be due to the density change or the photocarrier generation at the surface; this technique of "transient thermal reflectance" has been extended by Paddock and Eesley (1986) to the picosecond time resolution regime for monitoring thermal properties of thin films (~100Å) and of its interface conditions. Also, PT heating can cause changes in absorptivity in a sample; Zapka and Tam (1982a) have used a probe-beam absorption measurement to detect the

change in the Boltzmann molecular population distribution due to the PT heating of a gaseous sample.

III. CONCLUSION

We have given here an overview of the different versions of PT measurement and material characterizations which can be classified as follows:

(1) PT spectroscopy: in this class of application, the PT signal amplitude is measured for a range of optical excitation wavelength, producing an excitation spectrum. For quantitative interpretation, the PT generation efficiency must be known or at least kept fixed while the PT spectrum is obtained. Otherwise, the PT excitation spectrum is at best qualitatively showing the absorption peak positions.

(2) PT monitoring of de-excitation processes: here, the thermal decay branch is monitored to provide information on a competing decay branch. After optical excitation, four decay branches are generally possible: luminescence, photochemistry, photoelectricity, and heat that may be generated directly or through energy-transfer processes. For example, if luminescence and heat are the only two competing branches, and if the branching ratio can be controllably varied, PT monitoring of the heat branch can provide the quantum efficiency of luminescence.

(3) PT probing of thermoelastic and other physical properties of materials: various information can be obtained conveniently with the help of the optical generation of thermal waves or acoustic waves. Such information includes sound velocity, elasticity, temperature, flow velocity, specific heat, thermal diffusivity, thickness of a thin film, subsurface defects, delamination or air gap thickness, and so on.

(4) PT generation of mechanical motions: this is a small area of application now. PT effects can produce motions like liquid droplet ejection (Tam and Gill,

1982) or structural vibrations. Such effects can be enhanced by taking advantage of PT boiling, light-induced chain-reaction effects, or mechanical resonances.

In general, the choice of applying a PT source for heating rather than using a "Bunsen Burner" is justified by some of the following reasons: (1) PT heating can provide convenient, noncontact, and sensitive methods for detecting optical absorptions in matter, and is applicable for traditionally difficult samples (*e.g.*, highly opaque, transparent, or scattering); (2) information concerning de-excitation mechanisms and quantum yields can be obtained; (3) very localized or very rapid photothermal heating can be achieved to provide novel measurements or produce new effects with high spatial or temporal resolution, as well as providing subsurface and depth-profiling information.

This article has given an overview on PT probes with emphasis on the physical insights in probe-beam refraction techniques to detect PT refractive index gradients because of its quantitative, noncontact, and high-sensitivity nature. More detailed reviews of other PT probes have been given elsewhere, *e.g.*, reviews on photoacoustics (Rosencwaig, 1980; Patel and Tam, 1981; Tam, 1986) and photothermal radiometry (Kanstad and Nordal, 1986; Tam, 1985).

ACKNOWLEDGMENTS

This work is supported in part by the U.S. Office of Naval Research. The author thanks Heinz Sontag for his valuable contribution to this work.

TABLE I

The heating of a sample due to optical absorption can result in various photothermal effects and provide the corresponding detection techniques

Photothermal Effects	Detection Methods (applicable to sample S or to adjacent fluid F)
Temperature Rise	Laser calorimetry (S or F)
Pressure Change	Direct photoacoustic detection (S) Indirect photoacoustic detection (F)
Refractive Index Change (Thermal or Acoustic)	Probe-beam refraction (S or F) Probe-beam diffraction (S or F) Other optical probes (S or F)
Surface Deformation (Thermal or Acoustic)	Probe beam deflection (S) Optical interference (S)
Thermal Emission Change	Photothermal radiometry (S)
Reflectivity/Absorptivity Change	Transient thermal reflectance (S) Photothermal absorption monitoring (S or F)

REFERENCES

Abate, J. A., A. W. Schmid, M. J. Guardalben, D. J. Smith, and S. D. Jacobs, (1985), NBS Spec. Publ. (U.S.) **688**, 385.

Amer, N. M. 1983, J. de Phys. (Paris) Colloq. **C6**, 185.

Baumann, J., and R. Tilgner, 1985, J. Appl. Phys. **58**, 1982.

Bass, M., and L. Liou, 1984, J. Appl. Phys. **56**, 184.

Bass, M., E. W. Van Stryland, and A. F. Steward, 1979, Appl. Phys. Lett. **34**, 142.

Baumann, T., F. Dacol, and R. L. Melcher, 1983, Appl. Phys. Lett. **43**, 71.

Beaudoin, J. L., E. Merienne, D. Raphael, and M. Egee, 1986, Proc. SPIE - Int. Soc. Opt. Eng. **590**, 285.

Bialkowski, S. E. 1985, Appl. Opt. **24**, 2792.

Bialkowski, S. E. 1986, Spectroscopy **1**, 26.

Bialkowski, S. E., and G. R. Long, 1987, Anal. Chem. **59**, 873.

Boccara, A. C., D. Fournier, W. Jackson, and N. M. Amer, 1980, Opt. Lett. **5**, 377.

Bondarenko, A. N., Yu, B. Drobot, and S. V. Kruglov, 1976, Sov. J. Nondestr. Test. **12**, 655.

Bowers, J. E., 1982, Appl. Phys. Lett. **41**, 231.

Brilmyer, G. H., A. Fujishima, K. S. V. Santhanam, and A. J. Bard, 1977, Anal. Chem. **49**, 2057.

Busse, G. 1980, Infrared Phys. **20**, 419.

Busse, G., and P. Eyerer, 1983, Appl. Phys. Lett. **43**, 355.

Busse, G., and K. F. Renk, 1983, Appl. Phys. Lett. **42**, 366.

Calder, C. A., and W. W. Wilcox, 1980, Mater. Eval. **38**, 86.

Carslaw, H. S., and J. C. Jaeger, 1959, Conduction of Heat in Solids, 2nd Ed. (Clarendon Press, London).

Cielo, P. 1981, J. Acoust. Soc. Am. **25**, Suppl. 1 **70**, 546.

Cielo, P., G. Rousset, and L. Bertrand, 1986, Appl. Opt. **25**, 1327.

Coufal, H. 1984, Appl. Phys. Lett. **44**, 59.

Coufal, H., and P. Hefferle, 1985, Appl. Phys. A38, 213.

Crumbliss, A. L., P. S. Lugg, J. W. Childers, and R. A. Palmer, 1985, J. Phys. Chem., 89, 482.

Dadarlat, D., M. Chirtoc, and R. M. Candea, 1986, Phys. Status Solidi A 98, 279.

Dasch, C. J., and J. A. Sell, 1986, Opt. Lett. 11, 603.

Davidson, G. P., and D. C. Emmony, 1980, J. Phys. E 13, 92.

Davis, C. C. 1980, Appl. Phys. Lett. 36, 515.

Deem, H. W., and W. D. Wood, 1962, Rev. Sci. Instrum. 33, 1107.

Dovichi, N. J., T. G. Nolan, and W. A. Weimer, 1984, Anal. Chem. 56, 1700.

Eesley, G. L., B. M. Clemens, and C. A. Paddock, 1987, Appl. Phys. Lett. 50, 717.

Egee, M., R. Dartois, J. Marx, and C. Bissieux, 1986, Can. J. Phys. 64, 1297.

Field, R. S., D. E. Leyden, T. Masujima, and E. M. Eyring, 1985, Appl. Spectrosc. 39, 753.

Fotiou, F. K., and M. D. Morris, 1987, Anal. Chem. 59, 185.

Fournier, D., A. C. Boccara, and J. Badoz, 1981, Appl. Opt. 21, 74.

Fung, K. H., and H. B. Lin, 1986, Appl. Opt. 25, 749.

Glatt, I., Z. Karny, and O. Kafri, 1984, Appl. Opt. 23, 274.

Hata, T., T. Hatsuda, T. Miyabo, and S. Hasegawa, 1986, Jpn. J. Appl. Phys., 25, Supp. 25-1, 226.

Heritier, J. M. 1983, Opt. Commun. 44, 267.

Hutchins, D. A. 1983, Nondestr. Test. Commun. 1, 37.

Hutchins, D. A., and F. Nadeau, 1983, IEEE Ultrasonic Symposium Proceedings (IEEE, Piscataway, New Jersey), p. 1175.

Jackson, W. B., N. M. Amer, A. C. Boccara, and D. Fournier, 1981a, Appl. Opt. 20, 1333.

Jackson, W. B., N. M. Amer, D. Fournier, and A. C. Boccara, 1981b, in Technical Digest, Second International Conference on Photoacoustic Spectroscopy, Berkeley (Optical Society of America, Washington, D.C.), Paper WA3.

Jungerman, R. L., J. E. Bowers, J. B. Green, and G. S. Kino, 1982, Appl. Phys. Lett. 40, 313.

Jungerman, R. L., B. T. Khuri-Yakub, and G. S. Kino, 1983, J. Acoust. Soc. Am. 73, 1838.

Kanstad, S. O., and P. E. Nordal, 1986, Can. J. Phys. 64, 1155.

Karner, C., A. Mandel, and F. Traeger, 1985, Appl. Phys. A 38, 19.

Kasai, M., T. Sawada, Y. Gohshi, T. Watanabe, and K. Furuya, 1986, Jpn. J. Appl. Phys., 25, Suppl. 25-1, 229.

Kim, H. C. and H. K. Park, 1984, J. Phys. D 17, 673.

Klein, M. V. 1970, Optics (Wiley, New York).

Kliger, D. S., 1980, ACS Chem. Res. 13, 129.

Lai, H. M., and K. Young, 1982, J. Acoust. Soc. Am. 72, 2000.

Leite, R. C. C., R. S. Moore, and J. R. Whinnery, 1964, Appl. Phys. Lett. 5, 141.

Leung, W. P, and A. C. Tam, 1984a, Opt. Lett. 9, 93.

Leung, W. P., and A. C. Tam, 1984b, J. Appl. Phys. 56, 153.

Lin, H. B., and A. J. Campillo, 1985, Appl. Opt. 24, 422.

Long, G. R., and S. E. Bialkowski, 1985, Anal. Chem. 57, 1079.

Lopatkin, V. N., O. E. Sidoryuk, and L. A. Skvortsov, 1985, Kvantovaya Elektron. (Moscow) 12, 339.

Low, M. J. D., 1985, Spectrosc. Lett. 18, 619.

Loulergue, J.-C., and A. C. Tam, 1985, Appl. Phys. Lett. 46, 457.

Low, M. J. D., C. Morterra, A. G. Severdia, and M. Lacroix, 1982, Appl. Surf. Sci. 13, 429.

Low, M. J. D., C. Morterra, and A. G. Severdia, 1984, Mat. Chem. and Phys. 10, 519.

Low, M. J. D., C. Morterra, and J. M. Khosrofian, 1986, IEEE Trans. UFFC-33, 573.

Lucas, R., and P. Biquard, 1932, J. Phys. Radium 3, 464.

Mandelis, A., 1986, Rev. Sci. Instrum. 57, 617.

Mandelis, A., L. M. L. Borm, and J. Tiessinga, 1986, Rev. Sci. Instrum. 57, 622.

Mandelis, A., L. M. L. Borm, and J. Tiessinga, 1986, Rev. Sci. Instrum. 57, 630.

McDonald, F. A., G. C. Wetsel, Jr., and G. E. Jamies, 1986, Can. J. Phys. 64, 1265.

Miranda, L. C. M., 1983, Appl. Opt. 22, 2882.

Monchalin, J. P., 1986, IEEE Trans. UFFC-33, 485.

Morris, M. D., and K. Peck, 1986, Anal. Chem. 58, 811A.

Morterra, C., M. J. D. Low, and A. G. Severdia, 1985, Appl. Surf. Sci. 20, 317.

Mundy, W. C., J. E. L. Ermshar, P. D. Hanson, and R. S. Hughes, 1985, NBS Spec. Publ. (U.S.) 688, 360.

Murphy, J. C., and L. C. Aamodt, 1980, J. Appl. Phys. 51, 4580.

Murphy, J. C., and L. C. Aamodt, 1981, Appl. Phys. Lett. 38, 196.

Murphy, J. C., and G. C. Wetsel, 1986, Mater. Eval. 44, 1224.

Nakamura, H., K. Tsubouchi, and N. Mikoshiba, 1985, Jpn. J. Appl. Phys. 24, Suppl. 24-1, 222.

Nelson, K. A., and M. D. Fayer, 1980, J. Chem. Phys. 72, 5202.

Netzelmann, U., J. Pelzl, D. Fournier, and A. C. Boccara, 1986, Can. J. Phys. 64, 1307.

Nickolaisen, S. L., and S. E. Bialkowski, 1985, Anal. Chem. 57, 758.

Nordal, P. E., and S. O. Kanstad, 1979, Phys. Scr. 20, 659.

Nordal, P. E., and S. O. Kanstad, 1981, Appl. Phys. Lett. 38, 486.

Olmstead, M. A., and N. M. Amer, 1984, Phys. Rev. Lett. 52, 1148.

Olmstead, M. A., N. M. Amer, S. E. Kohn, D. Fournier, and A. C. Boccara, 1983, Appl. Phys. A 32, 141.

Opsal, J., A. Rosencwaig, and D. L. Willenborg, 1983, Appl. Opt. 22, 3169.

Paddock, C. A., and G. L. Eesley, 1986, J. Appl. Phys. 60, 285.

Palmer, C. H., R. O. Claus, and S. E. Fick, 1977, Appl. Opt. 16, 1849.

Patel, C. K. N., and A. C. Tam, 1981, Rev. Mod. Phys. 53, 517.

Rajakarunanayake, Y. N., and H. K. Wickramasinghe, 1986, Appl. Phys. Lett. 48, 218.

Roger, J. P., D. Fournier, A. C. Boccara, R. Noufi, and D. Cahen, 1985, Thin Solid Films 128, 11.

Rose, A., R. Vyas, and R. Gupta, 1986, Appl. Opt. 24, 4626.

Rosencwaig, A., 1980, Photoacoustics and Photoacoustic Spectroscoy (J. Wiley, New York).

Rosencwaig, A., J. Opsal, and D. L. Willenborg, 1983, Appl. Phys. Lett. 43, 166.

Rosencwaig, A., J. Opsal, W. L. Smith, and D. L. Willenborg, 1985, Appl. Phys. Lett. **46**, 1013.

Rosencwaig, A., J. Opsal, W. L. Smith, and D. L. Willenborg, 1986, J. Appl. Phys. **59**, 1392.

Rousset, G., F. Charbonnier, and F. Lepoutre, 1983, J. de Physique (Paris) Colloque **C6**, 39.

Sell, J. A. 1985, Appl. Opt. **24**, 3725.

Sell, J. A. 1987, Appl. Opt. **26**, 366.

Sell, J. A., and R. J. Cattolica, 1986, Appl. Opt. **25**, 1420.

Solimini, D., 1966, Appl. Opt. **5**, 1931.

Sontag, H., and A. C. Tam, 1985a, Appl. Phys. Lett. **46**, 725.

Sontag, H., and A. C. Tam, 1985b, Opt. Lett. **10**, 436.

Sontag, H., and A. C. Tam, 1986a, Can. J. Phys. **64**, 1121.

Sontag, H., and A. C. Tam, 1986b, IEEE Trans. UFFC-33, 500.

Sontag, H., A. C. Tam, and P. Hess, 1987, J. Chem. Phys. **86**, 3950.

Stegeman, G. I., 1976, IEEE Trans. Sonics Ultrason. SU-23, 33.

Suemune, I., H. Yamamoto, and M. Yamanishi, 1985, J. Appl. Phys. **58**, 615.

Sullivan, B., and A. C. Tam, 1984, J. Acoust. Soc. Am. **75**, 437.

Swofford, R. L., M. E. Long, and A. C. Albrecht, 1976, J. Chem. Phys. **65**, 179.

Tam, A. C. 1984, Appl. Phys. Lett. **45**, 510.

Tam, A. C. 1985, Infrared Phys. **25**, 305.

Tam, A. C., 1986, Rev. Mod. Phys. **58**, 381.

Tam, A. C., and G. Ayers, 1986, Appl. Phys. Lett. **49**, 1420.

Tam, A. C., and W. Gill, 1982, Appl. Opt. **21**, 1891.

Tam, A. C., and W. P. Leung, 1984, Phys. Rev. Lett. **53**, 560.

Tam, A. C., and H. Sontag, 1986, Appl. Phys. Lett. **49**, 1761.

Tam, A. C., H. Sontag, and P. Hess, 1985, Chem. Phys. Lett. **120**, 280.

Tam, A. C., and B. Sullivan, 1983, Appl. Phys. Lett. **43**, 333.

Tamor, M. A., and Hetrick, R. E., 1985, Appl. Phys. Lett. **46**, 460.

Tran, C. D., 1986, Appl. Spectrosc. **40**, 1108.

Uejima, A., M. Habiro, F. Itoga, Y. Sugitani, and K. Kato, 1986, Anal. Sci. **2**, 389.

Varlashkin, P. G., and M. J. D. Low, 1986a, Appl. Spectrosc. **40**, 507.

Varlashkin, P. G., and M. J. D. Low, 1986b Appl. Spectrosc. **40**, 1170.

Varlashkin, P. G., and M. J. D. Low, 1986c, Infrared Phys. **26**, 171.

Weimer, W. A., and N. J. Dovichi, 1985a, Appl. Spectrosc. **39**, 1009.

Weimer, W. A., and N. J. Dovichi, 1985b, Appl. Opt. **24**, 2981.

Wetsel, G. C., Jr., and J. B. Spicer, 1986, Can. J. Phys. **64**, 1269.

Whitman, R. L., and A. Korpel, 1969, Appl. Opt. **8**, 1567.

Winefordner, J. D., and M. Rutledge, 1985, Appl. Spectrosc. **39**, 377.

Williams, C. C., 1984, Appl. Phys. Lett. **44**, 1115.

Zapka, W., and A. C. Tam, 1982a, Opt. Lett. **7**, 86.

Zapka, W., and A. C. Tam, 1982b, Appl. Phys. Lett. **40**, 310.

Zapka, W., and A. C. Tam, 1982c, Appl. Phys. Lett. **40**, 1015.

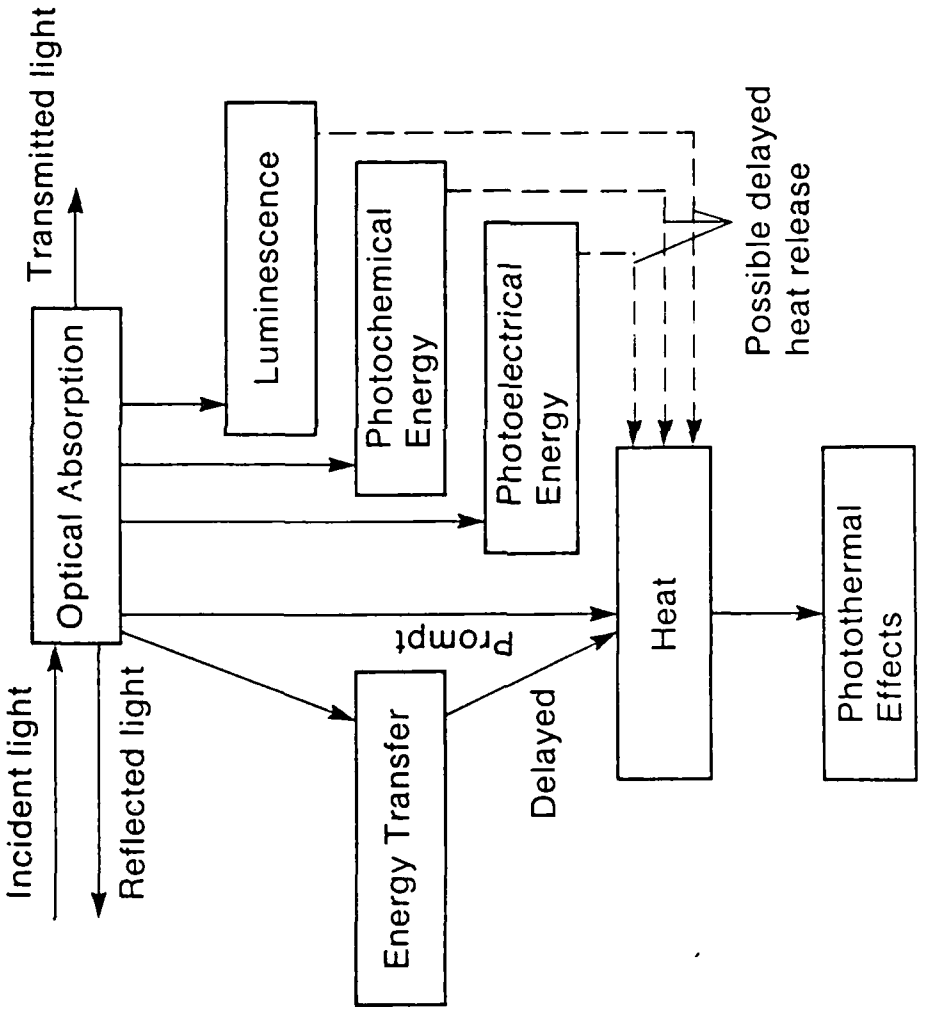

Figure 1. Block diagram to indicate the possible consequences of optical absorption, leading to "prompt" or "delayed" heat production in competition with other de-excitation

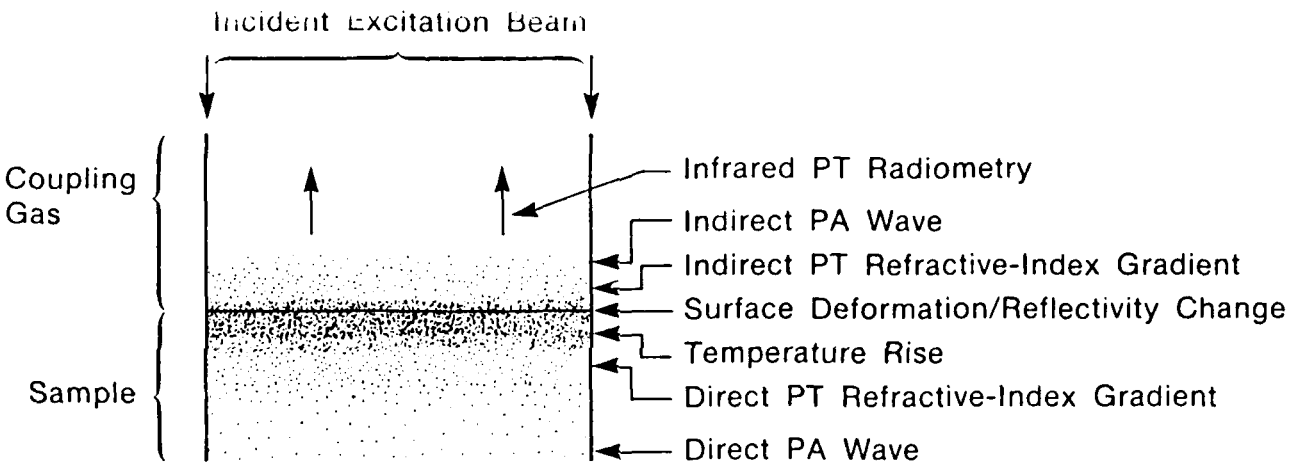

Figure 2. Common photothermal effects produced by modulated optical absorption in a sample. Direct effects observable in the sample and indirect effects observable in the transparent coupling medium adjacent to the sample are indicated.

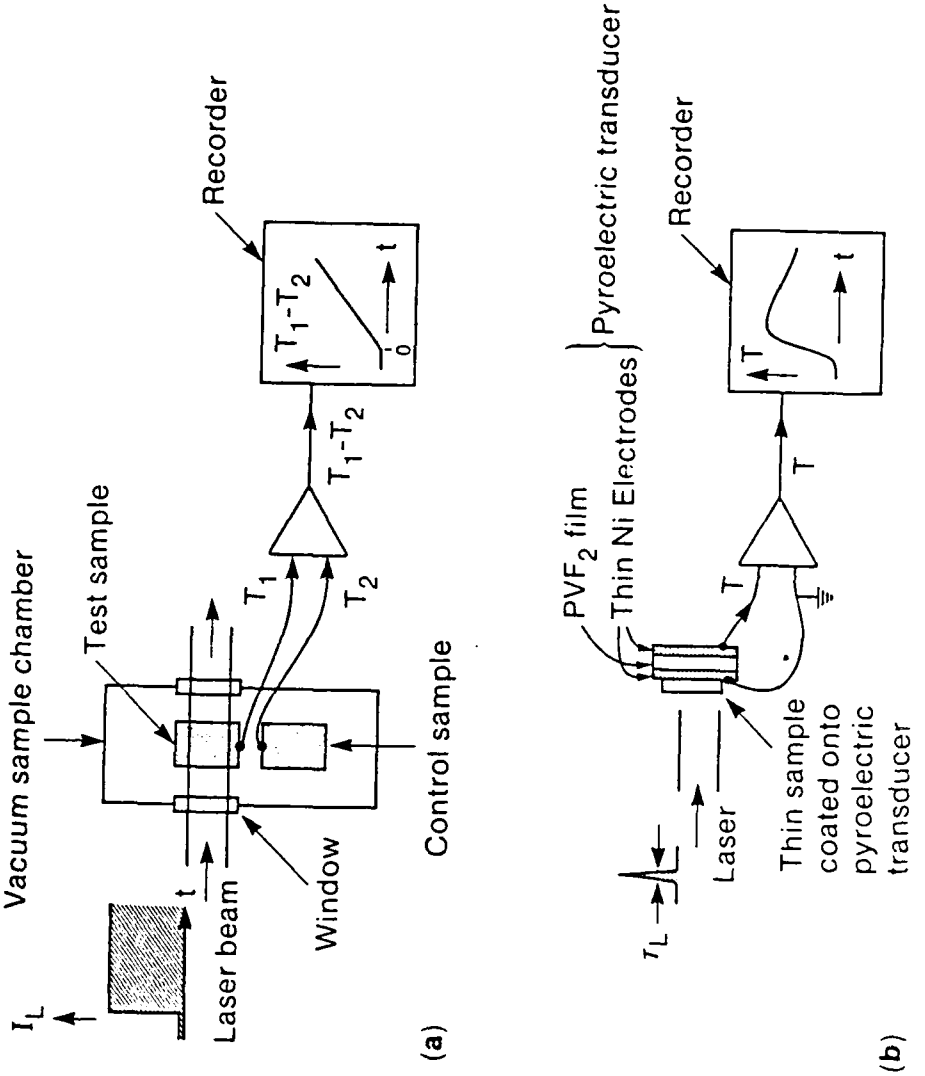

Figure 3. Examples of laser-calorimetry measurements: (a) step heating of an isolated sample; (b) pulsed heating of a thin sample in contact with a thin-film pyrometer.

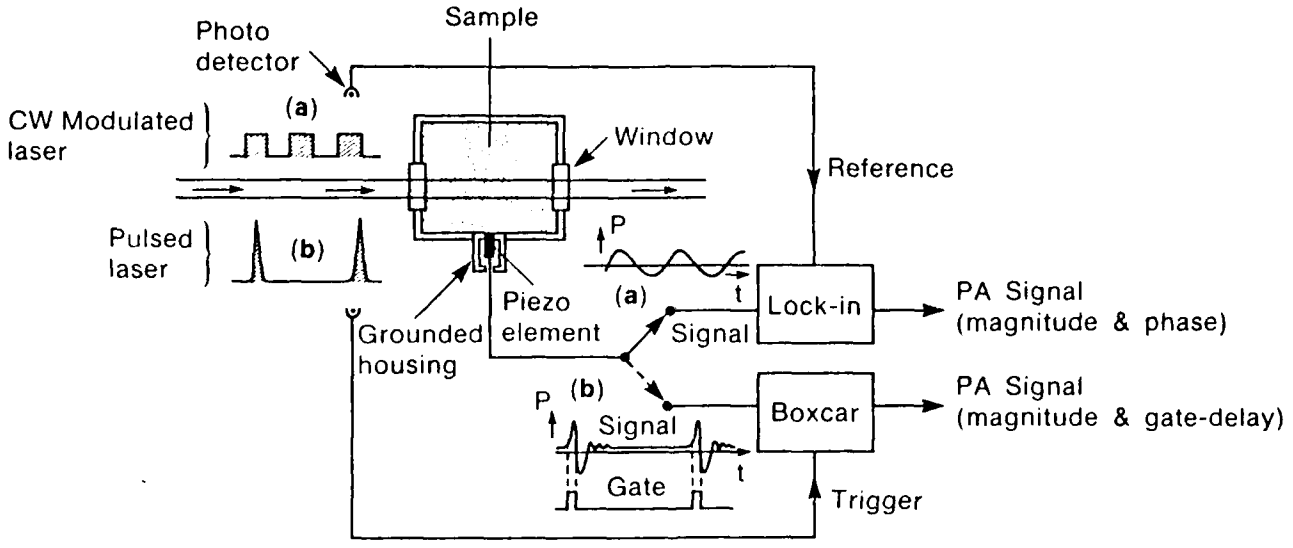

Figure 4. Schematics of direct PA measurement using (a) continuous modulated excitation, and (b) pulsed excitation.

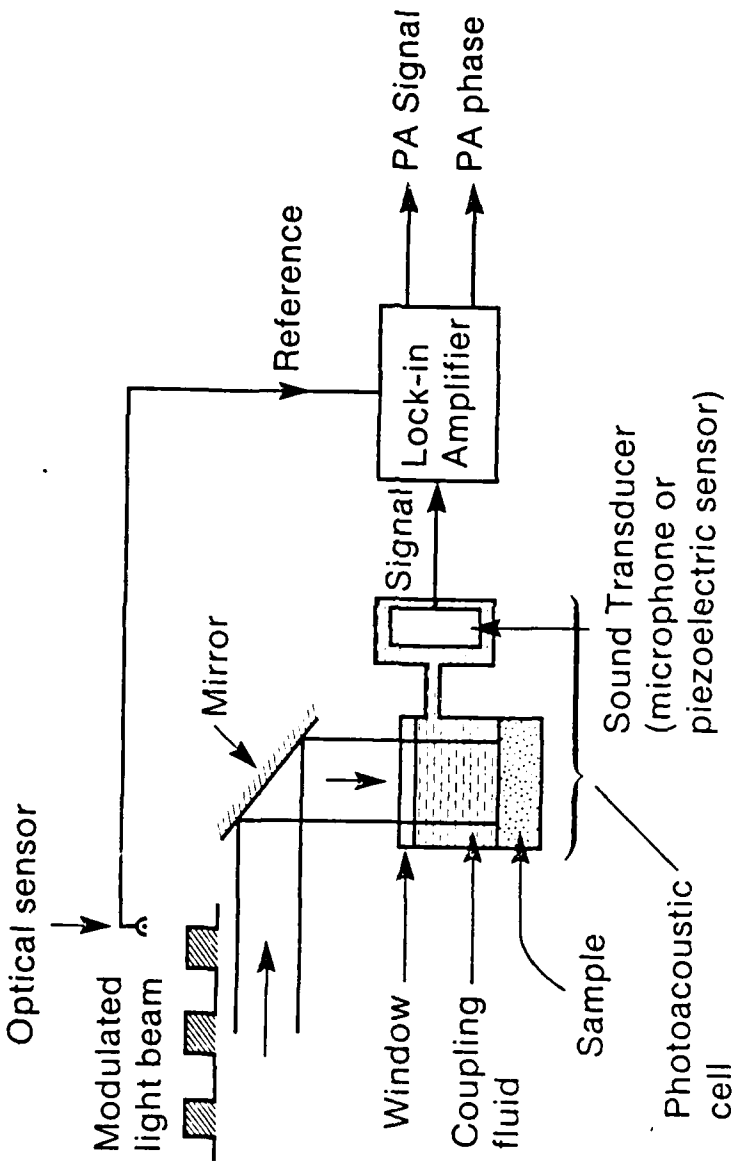

Figure 5. Schematic of indirect PA measurement using a continuous modulated excitation beam.

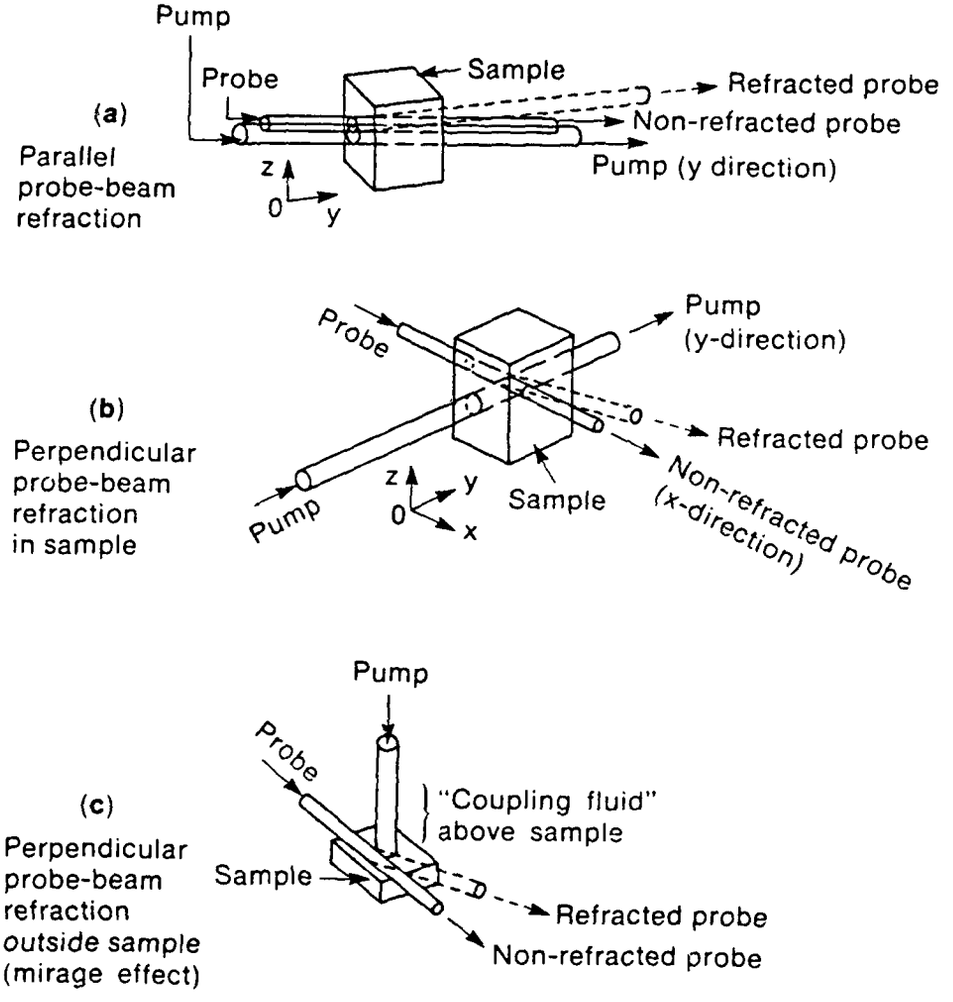

Figure 6. Examples of various PT probe beam refraction (PBR): (a) direct PBR in a sample for parallel pump and probe (the special case of concentric pump and probe is called "thermal lensing"); (b) direct PBR in a sample for perpendicular pump and probe; (c) indirect PBR in a coupling fluid adjacent to a sample for perpendicular pump and probe.

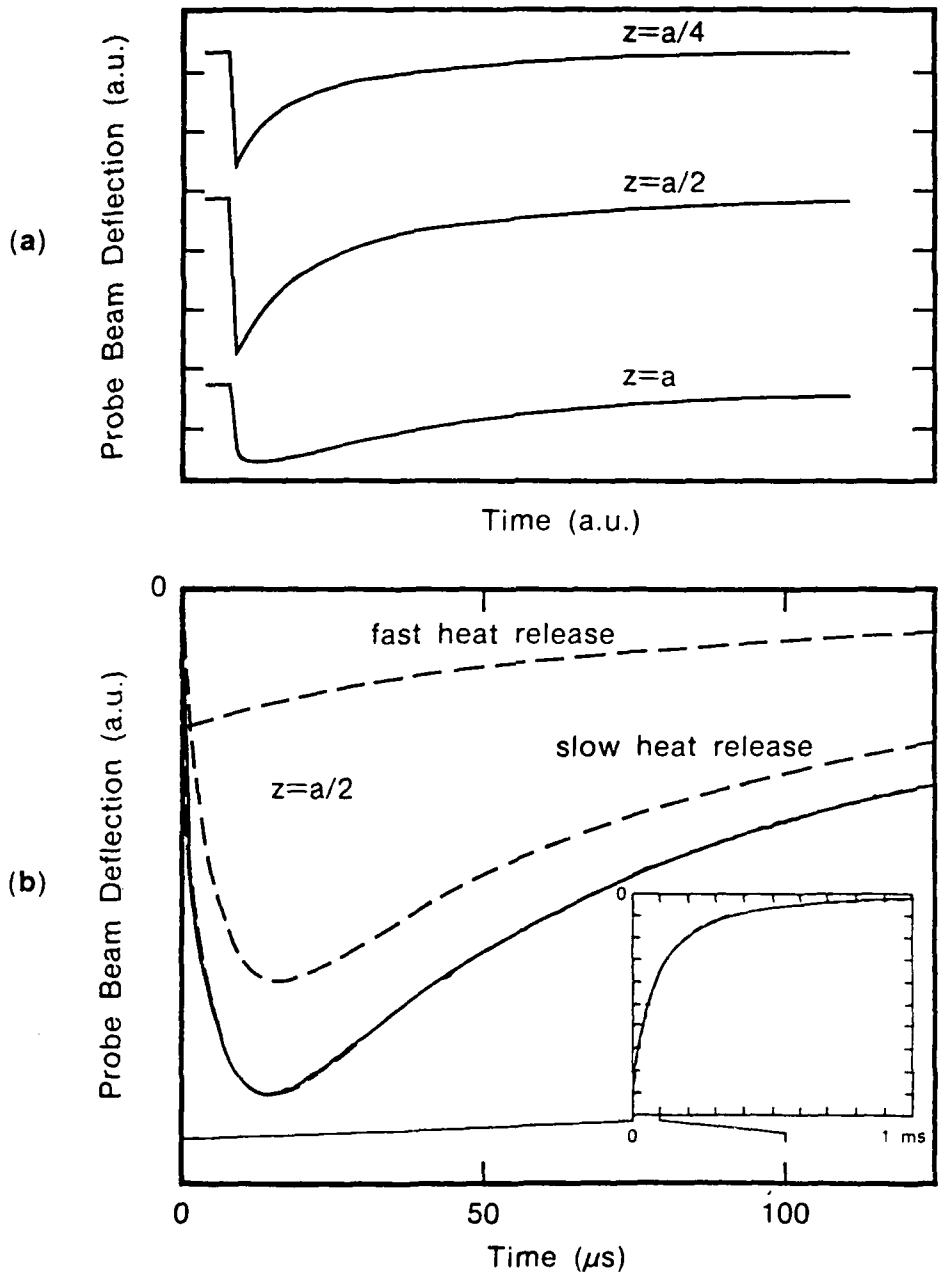

Figure 7. (a) Calculated perpendicular PBR signals for various separations z between the pump beam and the probe beam in a stationary sample with $\tau \approx 0$. The signal is largest for $z = a/2$, where the signal decay shape is also simple. (b) Calculated perpendicular PBR signal for $z = a/2$ in a stationary sample when the PT de-excitation has two time constants: a slow heat release component with a finite τ, and a fast heat release component with $\tau' \approx 0$. The resultant PBR signal has a delayed peak. The inset shows that the long-time decay is governed by thermal diffusion.

965-IBM-85

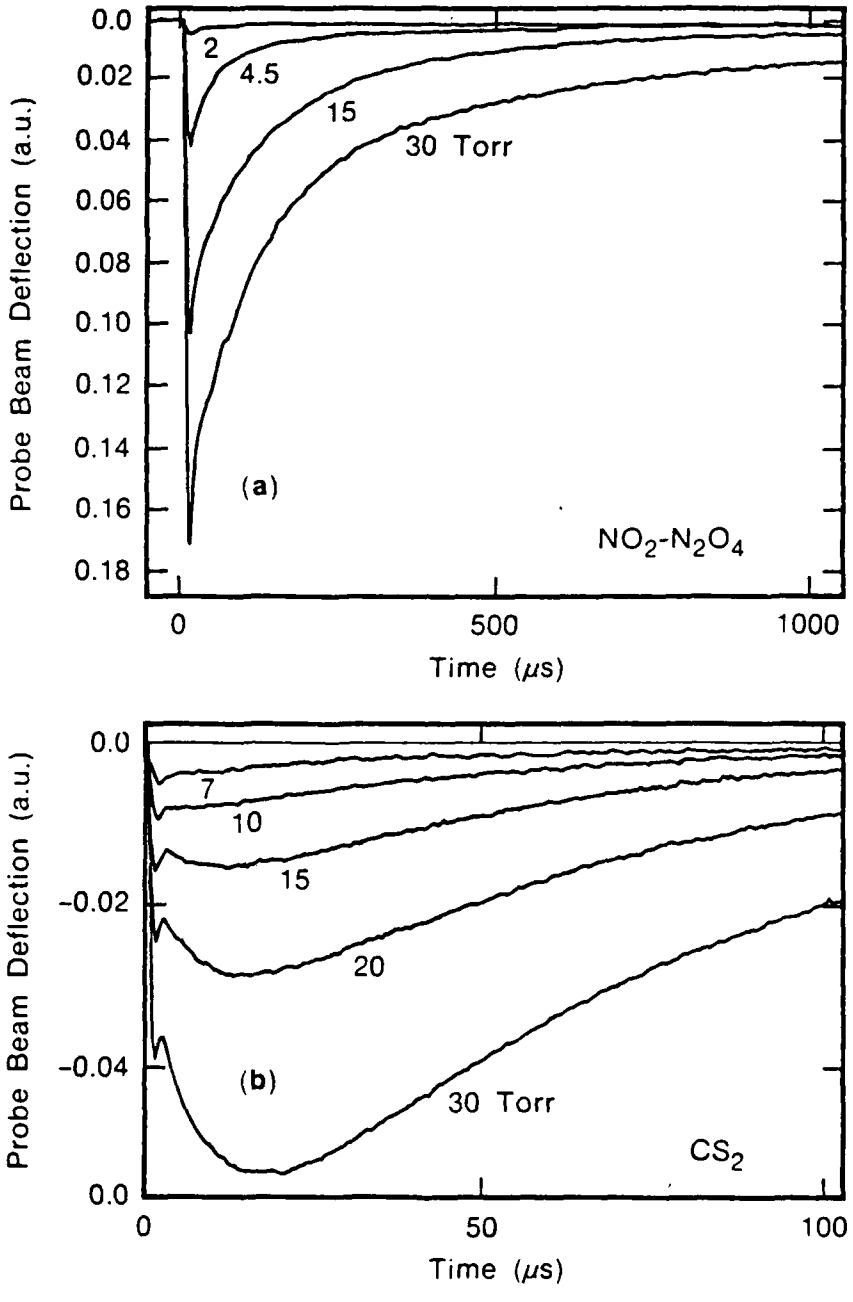

Figure 8. (a) Observed perpendicular PBR signals in a nitrogen dioxide gas of various pressure excited at 337 nm, with z = a/2, corresponding to the theoretical curve shown in Fig. 7a, middle trace. (b) Observed perpendicular PBR signals in a carbon disulphide gas of various pressures excited at 337 nm, with z = a/2; the higher pressure signals show the delayed peak indicated in Fig. 7b.

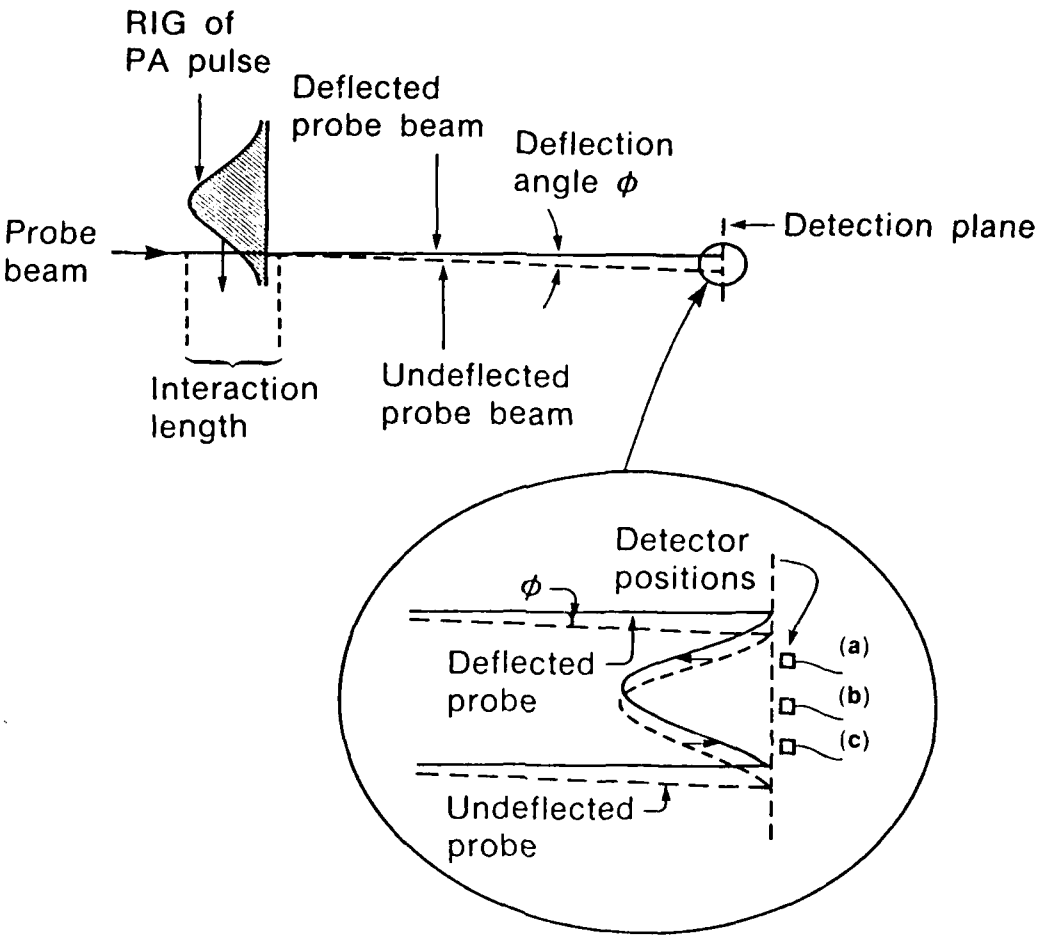

Figure 9. A probe-beam refraction (also called probe-beam deflection) method for noncontact transmission detection of PA pulses; transient deflection of a narrow collimated probe beam is caused by the PA refractive-index gradient (RIG). Three possible locations of a small detector, (a), (b), and (c) are indicated. The centered (b) positi[illegible]s nearly zero signal for a collimated probe undergoing small deflections, while [illegible] (c) give the maximum signals (with opposite phase) if the detectors are situate[illegible]he positions of maximum intensity slopes.

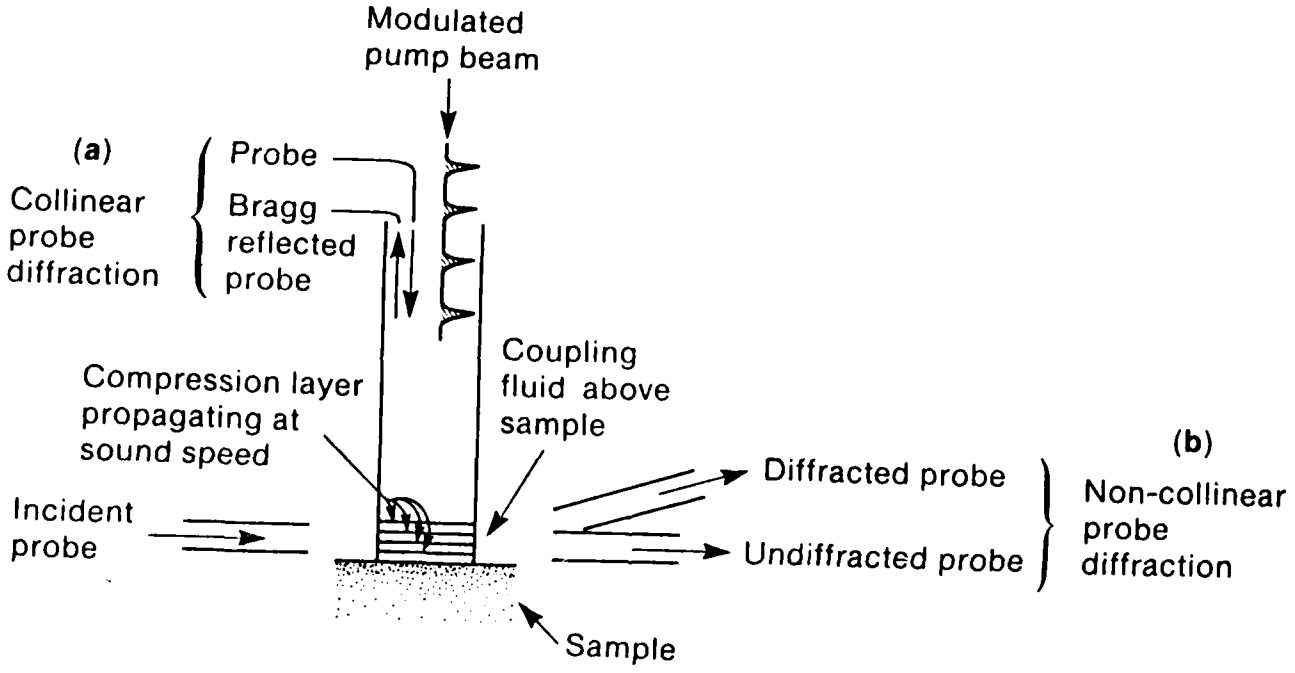

Figure 10. Examples of probe-beam diffraction for the case of a pump beam consisting of a train of short pulses incident on a sample, creating a layered refractive-index structure in the adjacent coupling fluid. The probe beam may be collinear or noncollinear with the pump beam, as indicated is (a) and (b), respectively.

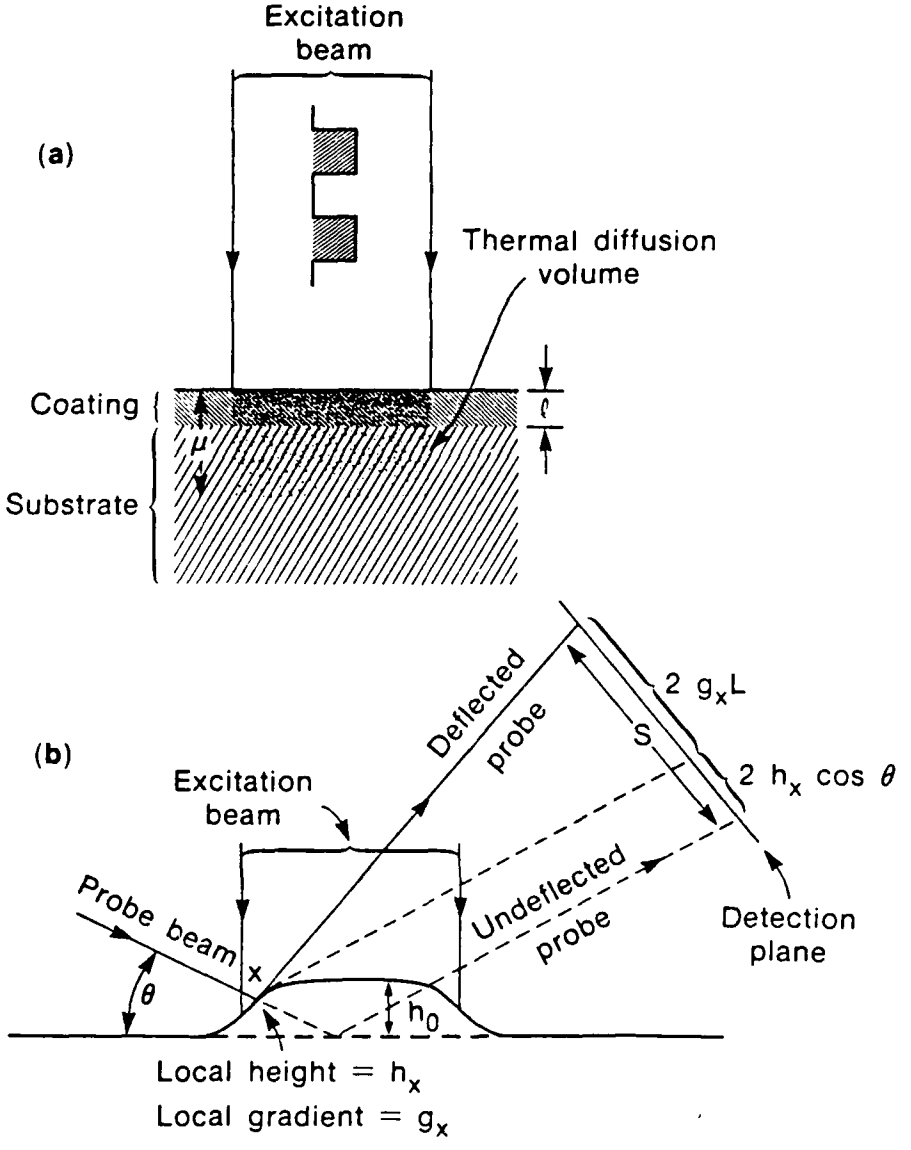

Figure 11. Photothermal displacement spectroscopy exemplified for the case of an absorbing layer of thickness l on a transparent substrate. (a) Schematic. (b) The probe beam incident at position X of the displaced surface (exaggerated in the figure) is deflected, and the displacement at the detection plane is $2h_x\cos\theta + 2g_xL$.

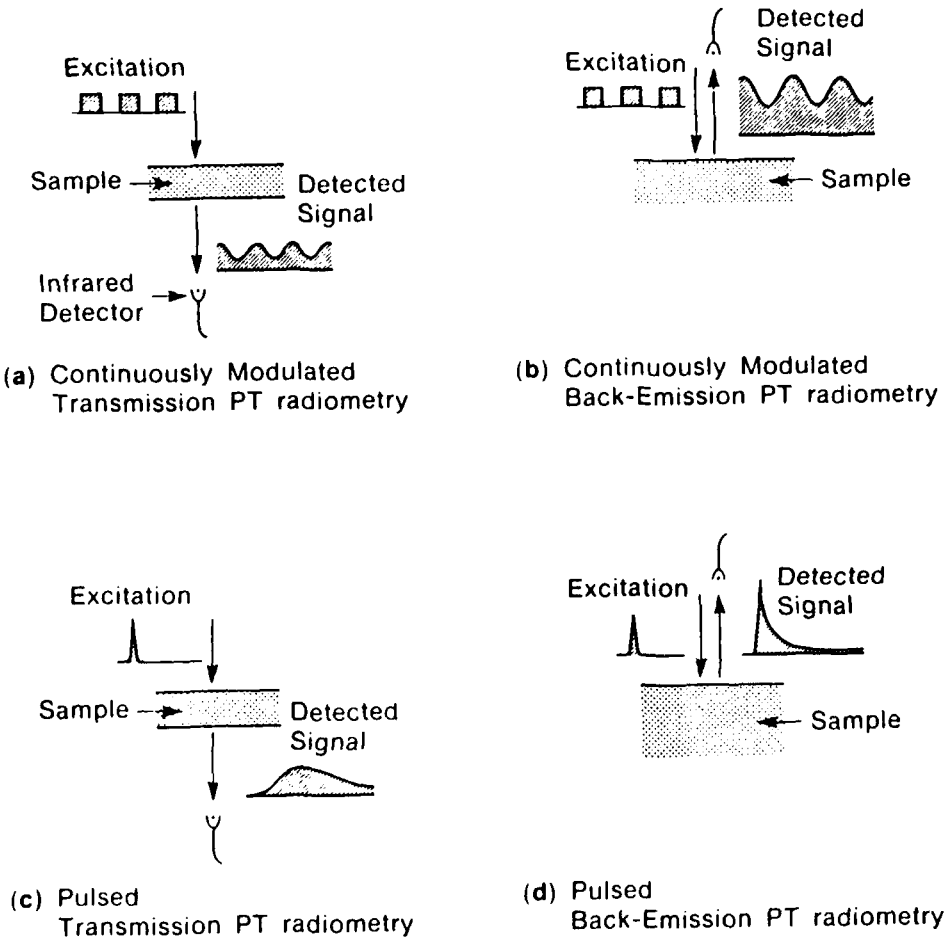

Figure 12. Variations of the photothermal radiometry techniques.